

Visualization and Biochemical Analyses of the Emerging Mammalian 14-3-3-Phosphoproteome*[§]

Catherine Johnson^{‡¶}, Michele Tinti^{‡¶}, Nicola T. Wood^{‡¶}, David G. Campbell[‡], Rachel Toth[‡], Fanny Dubois[‡], Kathryn M. Geraghty[‡], Barry H. C. Wong[‡], Laura J. Brown[‡], Jennifer Tyler[‡], Aurélie Gernez[‡], Shuai Chen[‡], Silvia Synowsky[‡], and Carol MacKintosh^{‡§}

Hundreds of candidate 14-3-3-binding (phospho)proteins have been reported in publications that describe one interaction at a time, as well as high-throughput 14-3-3-affinity and mass spectrometry-based studies. Here, we transcribed these data into a common format, deposited the collated data from low-throughput studies in MINT (<http://mint.bio.uniroma2.it/mint>), and compared the low- and high-throughput data in VisANT graphs that are easy to analyze and extend. Exploring the graphs prompted questions about technical and biological specificity, which were addressed experimentally, resulting in identification of phosphorylated 14-3-3-binding sites in the mitochondrial import sequence of the iron-sulfur cluster assembly enzyme (ISCU), cytoplasmic domains of the mitochondrial fission factor (MFF), and endoplasmic reticulum-tethered receptor expression-enhancing protein 4 (REEP4), RNA regulator SMAUG2, and cytoskeletal regulatory proteins, namely debrin-like protein (DBNL) and kinesin light chain (KLC) isoforms. Therefore, 14-3-3s undergo physiological interactions with proteins that are destined for diverse subcellular locations. Graphing and validating interactions underpins efforts to use 14-3-3-phosphoproteomics to identify mechanisms and biomarkers for signaling pathways in health and disease. *Molecular & Cellular Proteomics* 10: 10.1074/mcp.M110.005751, 1–15, 2011.

14-3-3s interact with hundreds of phosphoproteins inside all eukaryotic cells, including mammalian proteins that are deregulated in diabetes, cancer, platelet disorders, viral infections, and neurological disorders (1). Defining how the 14-3-3-binding phosphoproteome responds to extracellular stimuli and drugs therefore offers a rich source of signaling mechanisms, as well as potential biomarkers of disease and drug actions.

From the [‡]MRC Protein Phosphorylation Unit, College of Life Sciences, University of Dundee, James Black Centre, Dow Street, Dundee DD1 5EH, Scotland, UK

Received October 20, 2010, and in revised form, June 2, 2011

[✂] Author's Choice—Final version full access.

Published, MCP Papers in Press, July 1, 2011, DOI 10.1074/mcp.M110.005751

Recently, we collated data from the published studies that each report on interactions of 14-3-3s with one or a few targets (1). This exercise did more than simply organize data from multiple sources, but also helped reveal patterns. In particular, the collective data highlighted that 14-3-3 dimers frequently engage with two phosphorylated motifs on their targets, and phosphorylated 14-3-3-binding sites fall into subtypes that overlap with the specificities of different basophilic protein kinases such as PKA, Akt/PKB, p90RSK, PKCs, and AMPK. These specificities for 14-3-3s are consistent with the emerging roles for 14-3-3s in integrating cellular responses to insulin, growth factors, and nutrients (2–4).

As well as the low-throughput studies, high-throughput proteomics experiments have identified large pools of proteins that display affinity for 14-3-3s in extracts of human cells, rodent cells and tissues, bovine sperm, hydra, *Saccharomyces cerevisiae*, and plants (2–26). These experiments used a variety of 14-3-3 capture and release strategies, and were performed over a 6-year period with changing state-of-the-art in mass spectrometry. Some studies had additional goals such as distinguishing proteins that are phosphorylated and bind to 14-3-3s in response to insulin (2–4) and TNF- α (24), at different phases of the cell cycle (16), during apoptosis (27), and that interact with particular 14-3-3 isoforms (6, 14, 23, 28).

From their lists of proteins, each of these proteomics studies successfully selected one or a few proteins that were analyzed further according to the hypothesis guiding the study. However, the overall status of the accumulated datasets is unknown with respect to how many proteins have been validated as gold standards with precisely defined 14-3-3-binding phosphorylated sites. Moreover, the data are presented in a variety of formats (Excel, Word, pdf, JPEG) with no standard protein annotation system, which makes comparisons tedious. This is a pity because these data could be a valuable reference for ongoing projects to map dynamic changes in the 14-3-3-phosphoproteome in response to stimuli, drugs and disease.

We therefore collected the published datasets of 14-3-3-binding proteins from mammalian cells and tissues, and visualized them in VisANT graphs that are easy to explore, extend

and compare with other datasets. Comparing the commonalities and differences among experiments showed that there was only a modest representation of gold standard 14-3-3-binding proteins in the high-throughput data sets. This realization led us to validate the phosphorylation-dependent binding to further proteins that were selected from the graph to address questions of technical and biological specificity.

EXPERIMENTAL PROCEDURES

Protein Mapping—The interactions from three articles (14, 16, 28) were retrieved from the MINT database (29) whereas the interactions from one article (12) were from IntAct (30). Mint and IntAct store protein interactions according to the IMEx standard (<http://disber.net/imexdrupal/>), therefore from these two databases the 14-3-3 interacting proteins were retrieved with the UniProt accession id. Three articles (1, 3, 4) used the UniProt accession id and no further steps were required. Four articles (2, 7, 10, 20) used the IPI accession id, for which a python script was compiled from publicly available data sets (<ftp://ftp.ebi.ac.uk/pub/databases/IPI/current/>, ftp://ftp.uniprot.org/pub/databases/uniprot/current_release/knowledgebase/complete/) to create a dictionary and automatically map the IPI number into the UniProt accession id. Five articles used the GenBank id (6, 8, 9, 21, 26). To convert the GenBank id, a Python script was compiled with the BioPython module (31) to fetch the protein sequence from GenBank. The sequence was used as input for the NCBI blast service (blastp and Swissprot database) to retrieve the UniProt accession identity. The BioMart service at Ensembl was used to retrieve the human homologs of the mouse, rat and bovine UniProt accession identities (two proteins were defined as homologues if they share 80% amino acid identity).

Protein Annotation Clustering Analysis—From the 327 proteins discovered in more than two studies the 14-3-3, heterogeneous nuclear ribonucleoprotein, ribosomal, keratin, heat-shock, tubulin, actin, albumin, and ubiquitin proteins were removed from consideration, and the remaining 284 proteins were subject to clustering analysis with the DAVID resource using the medium classification stringency (32). The proteins annotated as mitochondrial were retrieved from the MitoMiner database (33) with only the GFP evidence, GO terms, and UniProt annotation considered. The proteins described as nucleolar were obtained from the Nucleolar Proteome Database (34). The interactions among the proteins in the cluster were retrieved with VisANT (35).

Western Blotting—Mouse monoclonal antibodies to detect KLC (MAB1617) and KHC (MAB1613) were from Chemicon International (Temecula, CA), mouse anti-GST from Sigma, mouse anti-VASP (pSer157) from Calbiochem (San Diego, CA), rabbit anti-14-3-3 (K19) from Santa Cruz (Santa Cruz, CA), GFP-Trap® coupled to agarose beads from Chromotek, horseradish peroxidase-conjugated secondary antibodies from Pierce, and AlexaFluor and IR Dye conjugated secondary antibodies for use with LiCor Odyssey were from Rockland and Pierce. The antibodies that recognize phosphorylated sites in DBNL, KLC2, and SMAUG2 were raised against the following synthetic phosphopeptides: CQKERAM(pS)TTSISS (residues 263 to 275, where pS is phosphoSer269 of DBNL, plus Cys for coupling: ref. S906B, 3rd bleed used in immunoblotting (IB)), CFLQKQL(pT)-QPETHF (residues 285 to 297, where pT is phosphoThr291 of DBNL, plus Cys for coupling: S907B, first, second, and third bleeds mixed for IB), VMGKVC(pT)QLLVSR (residues 478 to 490, where pT is phosphoThr484 of human SMAUG2; S395C, this antibody did not perform), SVQRTH(pS)LPVHSS (residues 636 to 648, where pS is phosphoSer642 of SMAUG2: S391C, first bleed for IB), CLRRSG(pS)-FGKLRD (Cys for coupling, and residues 540 to 551, where pS is phosphoSer545 of human KLC2: S099B, third bleed for IB) and

RMKRAS(pS)LNFLNKC (residues 576 to 588, where pS is phospho-Ser582 of KLC2, plus Cys for coupling: S136B, third bleed for IB). The peptides were conjugated via the added cysteine residues to bovine serum albumin and keyhole-limpet hemocyanin, mixed 1:1, and injected into sheep at Diagnostics Scotland (Penicuik, UK). The antibodies were affinity-purified on CH-Sepharose coupled to the cognate phosphopeptide in the Division of Signal Transduction Therapy, University of Dundee (DSTT). Sheep anti-SMAUG2 antibody was raised against purified bacterially-expressed GST-SMAUG2 (S214C, first bleed). Sheep anti-HA (hemagglutinin) and mouse anti-HA antibodies were raised against the peptide YPYDVPDYA.

Proteins transferred from SDS-polyacrylamide gels to nitrocellulose membranes were processed using enhanced chemiluminescent reagent (Amersham Biosciences) with HRP-conjugated secondary antibodies or Odyssey Infrared Imaging (LiCor) with AlexaFluor or IR Dye conjugates. Membranes were blocked in 5% Marvel dried milk powder in Tris-buffered saline (TBS) prior to detection. TBS contained 50 mM Tris-HCl pH7.5, 500 mM NaCl, and for TBS-T 0.1% (v/v) Tween-20 was included. Commercial antibodies were used in accordance with manufacturers' instructions, diluted in either 1% Marvel in TBS-T (w/v) or 50% TBS-T/50% LiCor Odyssey blocking buffer (v/v) (LiCor). Mouse anti-HA was used at 0.5 μ g/ml. Mouse anti-GST (supplied as ascites fluid, Sigma) was used at 1:3000. After initial tests of antibodies (supplementary Fig. S2), the anti-DBNL phosphospecific antibodies were used at 0.1 μ g/ml in the presence of 5 μ g/ml of the corresponding unphosphorylated peptide, anti-SMUAG2 phosphospecific antibodies at 1.0 μ g/ml with 10 μ g/ml unphosphorylated peptide, anti-SMAUG2 total antibody at 0.2 μ g/ml, and anti-KLC2 phosphospecific antibodies at 0.5 μ g/ml with 10 μ g/ml of the corresponding unphosphorylated peptide. ECL detection was performed according to the manufacturer's protocol. 14-3-3 overlays (using DIG (digoxigenin)-labeled 14-3-3 in place of primary antibody) were performed as previously described (2).

DNA Constructs—Recombinant DNA procedures, restriction digests, ligations and PCR, were performed using standard protocols. All PCR reactions were carried out using KOD Hot Start DNA polymerase (Novagen, Madison, WI). DNA sequencing was performed by The Sequencing Service, College of Life Sciences, University of Dundee (www.dnaseq.co.uk). Vectors for expression of proteins in mammalian cells were pCMV5 for expression of proteins with an N-terminal HA-tag, pcDNA5 FRT/TO modified to express proteins with an N-terminal GFP or GFP-tandem affinity purification (TAP) tag under a tetracycline inducible promoter, and the pGEX6P vector for expressing proteins with N-terminal GST tags in bacteria. In-house numbers for the clones in pCMV5 (unless specified otherwise) are ISCU (DU16772), DNBL (DU3456), LMO7 (DU7089), SMAUG2 (DU4266), KLC2 (DU595), KLC1J (DU16340), KLC1P (DU16263), and KLC1O (DU16369). Reference clones for GFP-tagged MFF and REEP4 are DU31774 and DU16797 respectively.

Culture, Transfection, and Lysis of HEK293 Cells—HEK293 cells were cultured at 37 °C in a 95% air/5% CO₂ water-saturated atmosphere and maintained in Dulbecco's modified Eagle medium, supplemented with 10% (v/v) fetal calf serum, 2 mM L-glutamine and 1% penicillin and streptomycin. At ~30% confluency, cells were transfected with 10 μ g plasmid DNA per 10-cm dish using 25 μ g polyethylenimine (PEI) and left for ~30 h. Cells were lysed in 0.3 ml lysis buffer containing 50 mM Tris-HCl pH7.5, 1 mM EGTA, 1 mM EDTA, 1% (w/v) Triton-X 100, 1 mM sodium orthovanadate, 50 mM sodium fluoride, 5 mM sodium pyrophosphate, 0.27 M sucrose, 0.1% (v/v) 2-mercaptoethanol, and one "Complete" protease inhibitor tablet per 50 ml.

Immunoprecipitations and GFP-Trap® Pulldowns—Cell extracts were pre-cleared on Protein G-Sepharose for 1 h at 4 °C. For pull-down of GFP-tagged proteins, supernatants were transferred to 5 μ l GFP-Trap® beads mixed with 25 μ l Sepharose for 1 h at 4 °C (unless

TABLE I
 Sources of data used for Figure 1

Sources of data	Species	Stimuli/conditions	Isolation procedure	Further information
Pozuelo Rubio et al. 2004 (20)	Human (HeLa suspension)	DMEM (10% FCS)	14-3-3 (BMH1/2)-Sepharose capture and ARAApSAPA peptide release	
Jin et al. 2004 (14)	Human (HEK293) stably expressing FLAG-14-3-3 γ	DMEM (10% FCS)	Anti-FLAG (M2 antibody) immunoprecipitation and FLAG or R18 peptide release	Also used other 14-3-3 isoforms In MINT
Meek et al. 2004 (16)	Human (HeLa)	Mitotic and interphase cells	Capture on GST-14-3-3 ζ and R18/11 peptide (RDLSWLDLEAN) release	In MINT
Benzinger et al. 2005 (28)	Human (TAP-14-3-3 σ HEK293)	DMEM (5% FCS)	TAP-14-3-3 σ purification	In MINT
Angrand et al. 2006 (10)	Mouse (TAP-14-3-3 ζ transgenic animals)	Perfused transgenic brains, livers and hearts	TAP-14-3-3 ζ purification	
Ewing et al. 2007 (12)	Human (HEK293)		Anti-FLAG (M2 antibody) immunoprecipitation and FLAG release	In IntAct
Puri et al. 2008 (21)	Bovine sperm	Not specified	GST-14-3-3 (YWHA)-Sepharose capture and R11 peptide release	
Yip et al. 2008 (4)	Mouse (3T3-L1 cells)	DMEM + and – insulin	14-3-3 β -Sepharose capture and SDS sample buffer release	
Dubois et al. 2009 (2)	Human (HeLa suspension)	DMEM + and – insulin	14-3-3 (BMH1/2) capture and ARAApSAPA release	Data from the dimethyl labelling experiment and the phosphopeptide identification were collated separately here
He et al. 2009 (7)	Human (293T)	none	14-3-3 protein epsilon Biotin tagging	
Larance et al. 2010 (3)	Mouse (L6 myotubes)	+ and – insulin	14-3-3 beta-Sepharose and SDS sample buffer release	
Zuo et al. 2010 (24)	Human (293T)	TNF- α	14-3-3 protein ϵ immunoprecipitation	
Liang et al. 2009 (25)	Human (293T)	none	14-3-3 protein ϵ	
Huang et al. 2010 (6)	Human NPC cells	none	TAP-14-3-3 σ	
Wilker et al. 2007 (23)	HumN U2OS cells	thymidine block	14-3-3 Σ immunoprecipitation	
Pozuelo Rubio 2010 (27)	Human (HeLa cells)	Ceramide	GFP-TAP-14-3-3 ζ	In MINT

stated otherwise). To immunoprecipitate HA-proteins, supernatants were mixed with 4 μ g anti-HA antibody/mg lysate for 1 h at 4 °C before addition of Protein G-Sepharose (30 μ l of a 50% slurry) for a further 1 h. Washes comprised 3 \times 1 ml in 500 mM NaCl, 50 mM Tris-HCl pH 7.5 and 2 \times 1 ml in 50 mM Tris-HCl pH 7.5, 0.5 mM EDTA, 0.1% 2-mercaptoethanol.

In Vitro Dephosphorylation of Isolated Cellular Proteins—For dephosphorylation reactions, GFP-Trap® beads (5 μ l, bulked out with 85 μ l Sepharose) were used to isolate GFP-tagged proteins from 1.5 mg lysate of transfected HEK293 cells that were grown in medium containing serum, and treated or not with calyculin A (CA; 50 nM for 15 min). Proteins had N-terminal tags, except ISCU and REEP4 that were C-terminally GFP-tagged to avoid interfering with N-terminal targeting regions, and KLC1J, which was HA-tagged and immunoprecipitated with anti-HA antibodies. After pulldown, beads were washed into reaction buffer (50 mM Tris-HCl pH7.5, 100 mM NaCl, 0.1 mM EGTA, 0.01% Brij-35 and 2 mM DTT) and split for three 50 μ l reactions. Proteins were dephosphorylated with 3 μ g lambda phosphatase in

the presence of 2 mM MnCl₂, plus 10 mM EDTA for the inhibited control, for 30 min at 30 °C. After further washing, beads were resuspended in SDS sample buffer, and analyzed for retention of copurified endogenous 14-3-3 proteins (K19 pan-14-3-3 antibody), and the ability of recombinant proteins to bind directly to 14-3-3s was examined by Far Western assay.

Generation of Stable Cell Lines Expressing GFP-TAP-SMAUG2 and TAP Purifications—Stable cell lines expressing GFP-TAP-SMAUG2 and GFP-TAP-SMAUG2-T484A/S642A under control of a tetracycline inducible promoter were generated in the Flp-In T-Rex-293 Cell Line according to the manufacturer's protocol (Invitrogen, Carlsbad, CA). The concentration of tetracycline that produced close to endogenous levels of SMAUG2 was 30 ng/ml for 16 h. Tandem affinity purifications were performed from 40 \times 15 cm dishes of HEK293 cells stably and inducibly expressing GFP-TAP-proteins using standard protocols (36).

Purification of Bacterially Expressed GST-tagged Proteins—GST-KLC2 fusion proteins were expressed from pGEX6P-KLC2 in *E. coli*

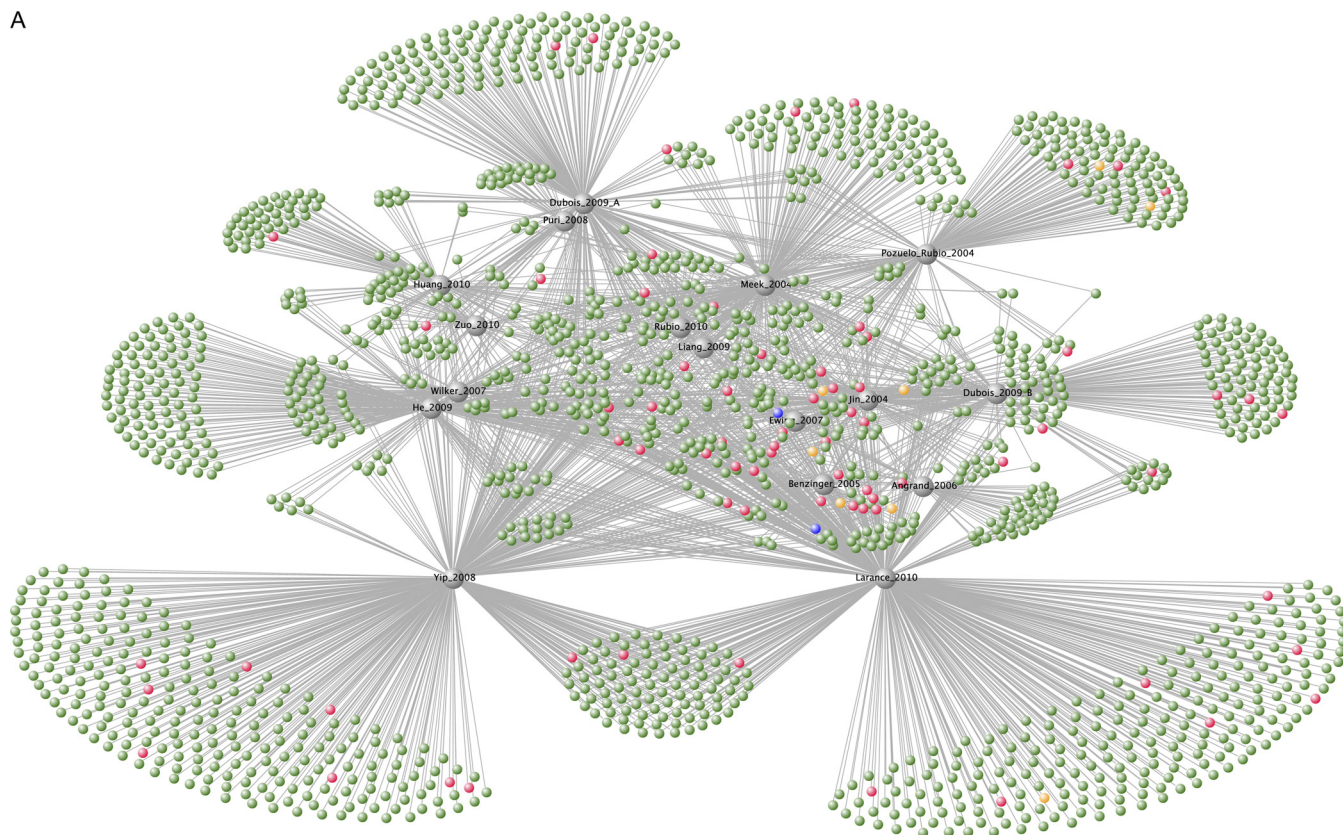


FIG. 1. **The 14-3-3 interactome.** A, A VisANT graph showing overlaps among the lists of proteins identified for their affinity for 14-3-3s in the proteomics screens listed in Table I, with data collated in [supplemental Table S1](#). Each paper is assigned a node in gray and lines connect the articles to the proteins, which are assigned as green nodes. Gold standard proteins for which 14-3-3-binding sites were reported in previous low-throughput studies (1) are in *red*, whereas in *orange* are proteins for which direct binding to 14-3-3 and relevant binding sites were characterized in this study. Isoforms of kinesin heavy chain are in *blue* to signify that these proteins bind to 14-3-3s indirectly via phosphorylated kinesin light chains (see text). The interactive version of this graph is available under 14-3-3 partners at our laboratory web page via <http://www.ppu.mrc.ac.uk/research>. B, The 14-3-3 binding proteome was clustered by molecular function or cellular localization as listed in [supplemental Table S3](#). Note that the MitoMiner database does not distinguish cytoplasmic proteins that interact with mitochondria from intrinsic mitochondrial proteins.

BL21 cells (Invitrogen) by induction with 250 μM isopropyl- β -D-thiogalactopyranoside at 37 $^{\circ}\text{C}$ for 16 h. GST-SMAUG2 proteins were expressed in *E. coli* DH5 α . Cells were sonicated, lysates centrifuged to clarify, and the GST fusion proteins purified by binding to glutathione Sepharose 4B beads (Amersham Biosciences), which were washed and proteins released in buffer containing 20 mM glutathione pH7.5. Purified proteins were dialyzed against 50 mM Tris-HCl pH7.5, 0.1 mM EGTA, 150 mM NaCl, 50% (v/v) glycerol, 0.03% Brij-35, 0.07% (v/v) 2-mercaptoethanol, 1 mM benzamide, 0.1 mM PMSF at 4 $^{\circ}\text{C}$ for 16 h.

Mass Spectrometry—Mass fingerprinting for protein identification was performed by in-gel digestion of Coomassie colloidal blue-stained protein gel bands with 5 $\mu\text{g}/\text{ml}$ trypsin and subsequent analysis of the tryptic peptides by LC-MS-MS on a Thermo LTQ-Orbitrap system. RAW files from Excalibur (Thermo) were processed by Raw2msm (37) to generate peaklists that were analyzed using the Mascot search engine (www.matrixscience.com) against the human International Protein Index database (82631 entries as of July 2009). Two missed cleavages were permitted and no known contaminants were excluded. The significance threshold was $p < 0.05$.

For identification of phosphorylated residues, the protein bands were digested for 4 h in 5 $\mu\text{g}/\text{ml}$ trypsin (followed by 16 h digestion with 5 $\mu\text{g}/\text{ml}$ Asp-N protease for the phosphoSer642-containing

SMAUG2 peptide). Peptides were analyzed by LC-MS-MS on an ABI 4000 Q-TRAP system using precursor ion scanning (38), in negative mode, searching for the $(\text{PO}_3)^-$ ion (-79 Da) allowing for ± 1 Da (38). This was followed by mass spectrometry in positive mode to perform MS2 analysis on the selected ions that were shown to have released the $(\text{PO}_3)^-$ ion. The resultant data files were searched against a database containing the appropriate sequence, using Mascot (version 2.2) run on an in-house server, (MRC_database_1, August 2009 containing 902 entries) with a peptide mass tolerance of 1.2 Da, a fragment mass tolerance of 0.8 Da, and with variable modifications allowing for phosphorylation of serine/threonine or tyrosine and for methionine oxidation or dioxidation. The significance threshold was $p < 0.05$ and the maximum missed cleavages permitted was four.

In Vitro Phosphorylation of KLC2—Purified recombinant protein kinases generated in the DSTT were MAPKAPK2, Brsk1, and Nuak2. MAPKAPK2 was activated by phosphorylation with SAPK2a at 30 $^{\circ}\text{C}$ for 45 min. Constitutively active Brsk1 and Nuak2 were generated by mutating the T loop threonine to glutamate (39). PKA was purified from bovine brain, and AMPK was purified from rat liver by Kevin Green in Grahame Hardie's group, University of Dundee. Kinase assays were performed in 50 mM Tris-HCl pH7.5, 100 μM EGTA, 0.1% (v/v) 2-mercaptoethanol in the presence of $[\gamma\text{-}^{32}\text{P}]\text{ATP}/\text{Mg}^{2+}$ (10 mM magnesium acetate, 0.1 mM ATP; specific radioactivity 300 to 1000

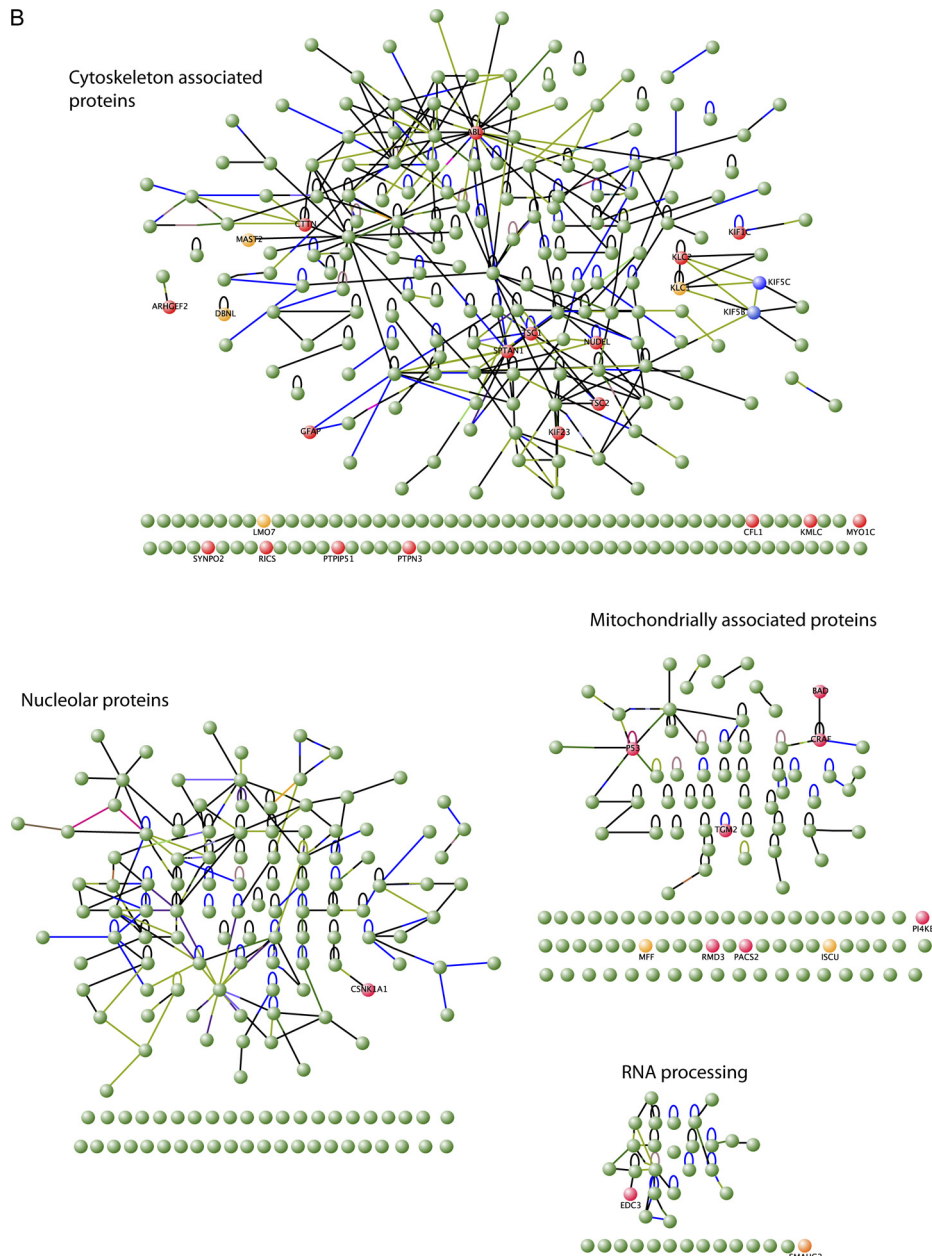




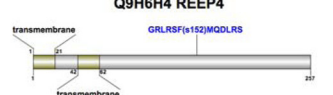
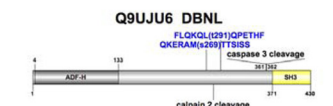
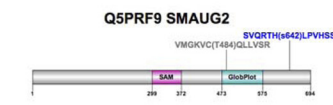
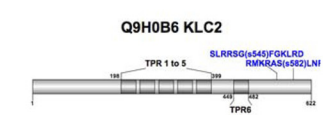
FIG. 1—continued

cpm/pmole) for 15 min at 30 °C. PKA and MAPKAPK2 were used at a specific activity of 1 U/ml. AMPK and related kinases were used in amounts that could incorporate ~6000 cpm into 50 μ l of 200 μ M AMARA peptide (AMARAASAAALARRR) in 15 min at 30 °C. Reactions were terminated by pipeting onto P81 papers, which were washed in 75 mM orthophosphoric acid, rinsed with acetone, dried and Cerenkov counted. *In vitro* phosphorylation of 5 μ g bacterially expressed GST-KLC2 was stopped with SDS-sample buffer, samples resolved by SDS-PAGE and Coomassie stained. Excised bands were subject to Cerenkov counting. GST-KLC2 fusion proteins (1 to 2 μ g) were also phosphorylated with 1 U/ml of AMPK *in vitro* for 30 min at 30 °C in the presence of either “cold” ATP/Mg²⁺ for Western blotting or [γ -³²P]ATP/Mg²⁺ for phosphopeptide mapping.

RESULTS

Collection and VisANT Visualization of Sixteen Published Mammalian High-throughput 14-3-3-Binding Studies—We unified the datasets from the sixteen high-throughput studies listed in Table I in which 1807 proteins from mammalian cell and tissue extracts were isolated by their affinity for 14-3-3s. The diverse annotation systems were transcribed so that each human protein was assigned a UniProt identifier. Mouse and bovine proteins were assigned UniProt identifiers for these species, and also the corresponding human homologues. The collated data is in [supplemental Table S1](#).

TABLE II
Sites on mammalian proteins whose mutation prevents 14-3-3 binding

Uniprot accession and protein name	Protein structures drawn using Domain Graph, version 1.0.5 (52) with phosphorylated 14-3-3-binding sites in blue. Residues whose mutation affects 14-3-3-binding, but are not known to be phosphorylated are in grey type.	Conservation of phosphorylated to 14-3-3 binding sites	Notes on protein
Q9GZY8 (MFF) mitochondrial fission factor	Q9GZY8 MFF 	In mammalian proteins, uncertain in <i>Xenopus</i> , fish, and insects.	Tethered via C-terminus on cytoplasmic face of outer mitochondrial membrane, and plays a role in fission of mitochondria and peroxisomes (53).
Q9H1K1 (ISCU) mitochondrial iron-sulphur cluster assembly enzyme	Q9H1K1 ISCU 	Both sites in mammalian ISCU, but not obvious in <i>Xenopus</i> , fish, birds and yeast.	ISCU is expressed from a nuclear gene and imported into mitochondria where it functions in Fe-S cluster assembly (54). Mutation of ISCU causes myopathy with exercise intolerance Swedish type, in which mitochondrial Fe-S proteins and oxidative metabolism are impaired, and there is lactic acidosis (44, 45, 55).
Q9H6H4 (REEP4) receptor expression-enhancing protein 4	Q9H6H4 REEP4 	Conserved in REEP1, 2, 3 and 4 in humans and other mammals.	Tethered via transmembrane domains at N-terminus to cytoplasmic face of endoplasmic reticulum. (Earlier reported to be attached to mitochondria). Multiprotein family, of which the REEP1 gene product is mutated in a form of hereditary spastic paraplegia (9, 26).
Q9UJU6 (DBNL) debrin-like protein	Q9UJU6 DBNL 	Both sites in mammalian DBNL, but not DBNL in other vertebrates, insects, plants and fungi.	Also called SH3P7/mAbp1/HIP-55. Involved in actin-mediated endocytosis and other actin-mediated membrane events. The ADF-H domain interacts with ADF-H, and the SH3 domain with various membrane-associated proteins. A calpain 2 site whose cleavage affects dorsal ruffling of cells lies between the 14-3-3 binding sites (46).
Q5PRF9 (SMAUG2) Smaug homologue 2	Q5PRF9 SMAUG2 	Both sites are in vertebrate SMAUG2, but not insect proteins. Also in mammalian SMAUG1.	The SAM domain recognizes Smaug recognition elements in the 3'-UTR of target mRNAs. While Smaug is best characterized for repressing and deadenylating maternal mRNAs in <i>Drosophila</i> (56), the insect protein does not contain the 14-3-3-binding sites identified here, and in human only the related Smaug1 protein has been studied previously (57).
Q07866 (KLC2) kinesin light chain 2	Q9H0B6 KLC2 	Both sites are in mammalian KLC2, 3 and 4, and variants of KLC1 that express exons 16 and 17.	In kinesin motor that carries cargo from nucleus towards periphery of cells. Kinesin is a heterotetramer of two heavy and two light chains. The pairs of light chains in each complex are reported to be the same isoform. Light chains are implicated in regulation of the motor function of the heavy chain and/or mediating interactions of the kinesin with its cargoes in a KLC-isoform specific manner (47).

We chose VisANT (<http://visant.bu.edu>) to visualize and analyze the collated mammalian 14-3-3-phosphoproteome data because it is free, flexible and relatively easy to use (35). The VisANT graph in Fig. 1A displays each 14-3-3-phosphoproteomics study as a gray node connected to proteins in green (and other colors see later text). The interactive version of the graph is available from our laboratory website (<http://www.ppu.mrc.ac.uk/research/?pid=5&sub1=14-3-3%2BPartners>). The “relaxed elegant” VisANT rule was applied, which dynamically places each protein so that those that feature most frequently make their way to the center (comprising 327 proteins that are shared by at least three studies), whereas proteins identified in only one experiment (a total of 1139) fan toward the outside. Tension in the connecting lines means that when studies have a protein in common the lines shorten, pulling the two studies closer together, which means that the layout reflects patterns in the data.

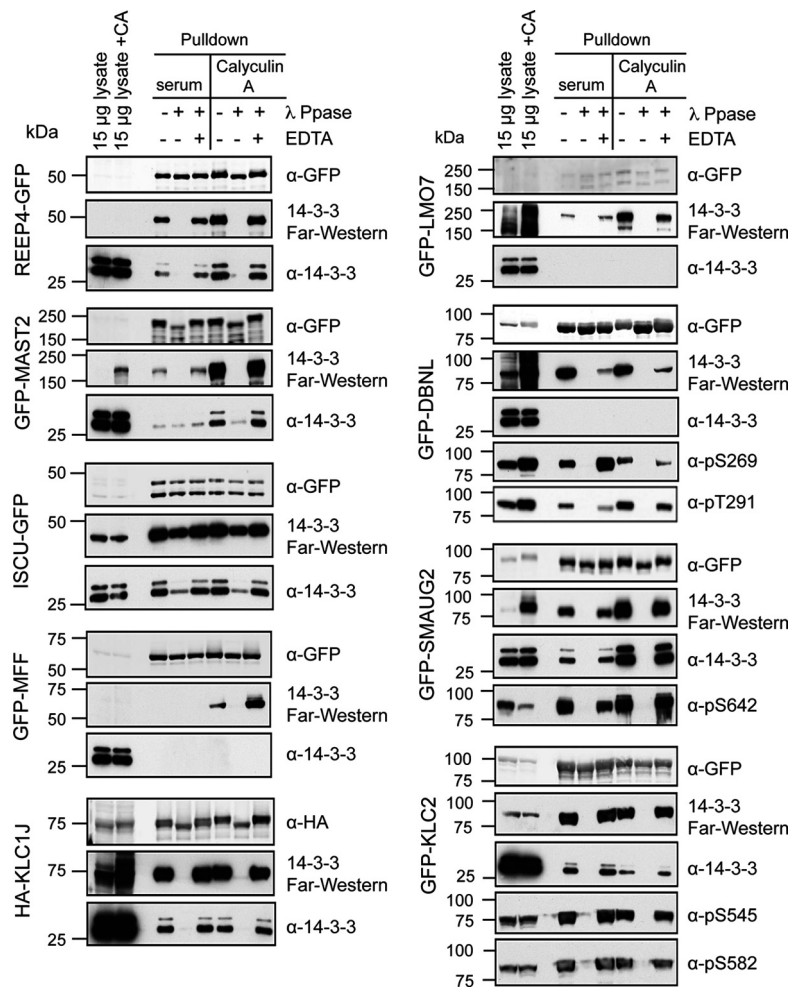
Update and Assessment of the Gold Standard Status of the High-throughput 14-3-3-Binding Studies—In January 2010, 14-3-3 binding sites had been reported for 146 mammalian proteins (Table II of (1)), mainly deduced because their mu-

tagenesis decreased 14-3-3 binding. We updated this table by searching PubMed for papers identifying proteins that bind directly to 14-3-3. These recent interactions up to August 2010 and the protein interactions in the papers listed in reference (1) were deposited in the MINT database according the light curation standards (29). We visualize and annotate this dataset in [supplemental Fig. S1](#) and [supplemental Table S2](#) respectively.

Of the 152 proteins in these low-throughput studies, 76 (50%) were not discovered in the high-throughput experiments, 30 (20%) are unique to one or other high-throughput experiment, whereas 46 (30%) appear in at least two and are central in the graph (red nodes in Fig. 1A).

Therefore, most proteins in the high-throughput experiments are unassigned with respect to whether they are phosphoproteins that dock directly onto 14-3-3s, bind to 14-3-3s indirectly within larger protein complexes, or are nonspecific contaminants. With a view to extending the “gold standard” data set, we therefore considered criteria that might help preselect useful proteins for further validation.

FIG. 2. Direct phosphorylation-dependent interactions of 14-3-3s with selected proteins. Tagged recombinant proteins were isolated from lysates of transfected HEK293 cells that were grown in medium containing serum, and treated or not with calyculin A (CA) as indicated. Proteins were dephosphorylated with lambda phosphatase, or not, when the phosphatase was inhibited with EDTA, and analyzed for retention of co-purified endogenous 14-3-3 proteins (K19 pan-14-3-3 antibody). The ability of recombinant proteins to bind directly to 14-3-3s was examined by Far Western assay. DNBL, KLC2 and SMAUG2 were also analyzed by Western blotting with the indicated phospho-specific antibodies, which were characterized in [supplemental Fig. S2](#).



Position on the Graph—Whether a protein is central or peripheral on the VisANT graphs does not itself allow value judgements about its likely 14-3-3-binding status, as indicated by the distribution of gold standards (red nodes) both in the center and on the outside of Fig. 1A. Experiments that have uniquely identified many proteins might be more comprehensive, contain more contaminants than other studies, and/or have selected particular proteins because of the 14-3-3 isoform used as the affinity ligand, phosphorylation status of proteins in the cells, or experimental protocol. Conversely, central frequently identified proteins could be either common contaminants or true 14-3-3-binding proteins found in many cell types and whose peptides perform well in mass spectrometers. Because we aim to define a larger set of gold standards with reliable mass spectrometry signals, we chose mainly proteins in the center of the graph for further experimental evaluation.

Biological and Technical Questions Arising from Fig. 1—The proteins featured in Fig. 1 include proteins linked to diseases, proteins with well-defined functions, many of unknown function, and proteins from different cellular compartments. We noticed that the lists of 14-3-3 affinity-purified proteins feature

many unvalidated cytoskeletal proteins (Fig. 1B), raising concerns about whether these proteins have been isolated via direct interactions with 14-3-3s or in cytoskeletal conglomerates. We therefore selected cytoskeletal-associated proteins for further analysis. Unvalidated mitochondrial and endoplasmic reticulum proteins also feature in the high-throughput studies (Fig. 1B), raising concerns about the relevance of these interactions with the 14-3-3s, which are generally considered to be nuclear and cytoplasmic proteins.

Here, we present experimental data on the 14-3-3-binding properties of proteins listed in Table II, as well as the mitochondrial protein p32/gC1qR, and three cytoskeletal regulators, namely LMO7, the protein kinase MAST2 and kinesin light chain 1J, which were selected after considering the above criteria.

Identification of Proteins that Bind Directly to 14-3-3 in a Phosphorylation-dependent Manner—Tagged forms of the selected proteins were expressed in HEK293 cells, and when extracted from transfected cells most of these proteins co-immunoprecipitated with endogenous 14-3-3 proteins from the cell lysates, and/or could also bind directly to 14-3-3 in a Far-Western assay (Fig. 2). The 14-3-3 binding signals of

REEP4 and MAST2 increased when cells were treated with the protein phosphatase inhibitor calyculin A, indicating that their 14-3-3-binding sites were not fully phosphorylated in cells growing under the standard conditions. No 14-3-3-binding signal was detected for the mitochondrial p32/gC1qR, although a proportion of cellular p32/gC1qR can be specifically coimmunoprecipitated with 14-3-3s from cells, indicating that this protein may bind 14-3-3 indirectly via an intermediary phosphoprotein (data not shown). For those proteins that did bind to 14-3-3 directly, their interactions were abolished or markedly reduced by incubation with lambda phosphatase, but not when the protein phosphatase was inhibited with EDTA (Fig. 2). In summary, ISCU, MFF, REEP4, KLC2, KLC1 isoform J (the relevance of this isoform is explained later), LMO7, MAST2, DBNL, and SMAUG2 display direct phosphorylation-dependent interactions with 14-3-3 (Fig. 2).

Identification of Phosphorylated Residues Whose Mutation Prevents Binding of 14-3-3s to Target Proteins

ISCU, MFF, REEP4, and DNBL—For ISCU, MFF, REEP4, and DNBL, phosphorylated serine/threonine residues that resemble potential 14-3-3-binding sites had been reported in the literature (<http://phospho.elm.eu.org/> and <http://www.phosphosite.org>). We found that substituting alanine for the following phosphorylatable residues prevented binding of the recombinant proteins to 14-3-3: Ser14 of ISCU, Ser157 (but not Ser179) of MFF, and Ser269 and/or Thr291 of DBNL (Fig. 3). The use of phosphospecific antibodies raised against phosphoSer269 and phosphoThr291 of DBNL, showed that the mutation of one of these residues did not affect phosphorylation of the other (Fig. 2, Fig. 3, and [supplemental Fig. S2](#)), and these data therefore suggest that a 14-3-3 dimer docks onto both phosphorylated residues. In the case of REEP4, mutation of Ser152 to alanine decreased, but did not abolish 14-3-3 binding to this protein (Fig. 3). In addition, it was noticed that Ser29 on ISCU looks like a potential 14-3-3-binding site, and mutation of this residue abolished binding to 14-3-3 (Fig. 3), although we have no direct evidence that Ser29 on ISCU is phosphorylated.

SMAUG2—The binding of 14-3-3 to SMAUG2 was unaffected by mutating known phosphorylated residues on SMAUG2 (<http://phospho.elm.eu.org/> and <http://www.phosphosite.org>) and additional phosphorylated residues that we identified on this protein by mass spectrometric analyses. The mutations tested were Ala substitutions of Ser236, Ser238, Thr405, Thr406, Thr407, Thr606, Ser607, and Ser592 (data not shown). We therefore used truncations to narrow down the 14-3-3-binding site(s). Loss of residues 671 to 694 had no impact on 14-3-3-binding, whereas loss of 432 to 694 prevented 14-3-3-binding (Fig. 4A). Within residues 432 to 694 there was a potential 14-3-3-binding site at Ser642, and indeed a Ser642Ala mutation decreased binding of SMAUG2 to 14-3-3 (Fig. 4B). If (phospho)Ser642 is one binding site, there has to be a further site within residues 432 to 621 because a truncated protein comprising residues 1 to 621 can

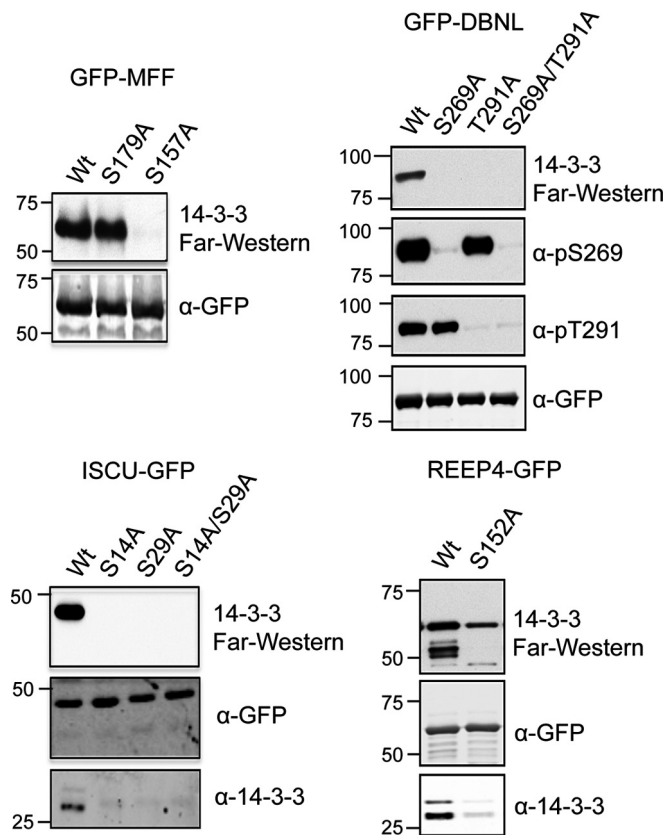


Fig. 3. Phosphorylated sites whose mutation prevents 14-3-3 binding. GFP-MFF, GFP-DBNL, ISCU-GFP, and REEP4-GFP, and the indicated single and double alanine mutants of these proteins, were immunoprecipitated on GFP-TRAP® beads from transfected cells, and tested for their ability to bind directly to 14-3-3s in Far Western assays, and by copurification with endogenous 14-3-3s from the cell extracts. For ISCU, the upper GFP signal is the intact protein (which runs as a doublet in Fig. 2) and a fainter lower band is the processed form that lacks the N-terminal signal sequence. For GFP-DBNL, the immunoprecipitated proteins were also examined for phosphorylation of Ser269 and Thr291 using phosphospecific antibodies, as characterized in [supplementary Fig. S2](#).

bind 14-3-3, albeit to a lesser extent than full-length protein (Fig. 4A). Of the twenty-four serine and threonine residues between 432 and 621 four have basic residues in the -3 or -4 positions, with one also having a proline at $+2$. These features are typical of 14-3-3 binding sites. When single and double mutations of these residues were tested, only the Thr484Ala/Ser642Ala double mutation abolished 14-3-3 binding (Fig. 4B).

At this stage however, there was no evidence that either Thr484 or Ser642 of SMAUG2 are actually phosphorylated in cells. Therefore, sheep were injected with conjugated phosphopeptides to raise antibodies that would recognize phosphorylated Thr484 and Ser642, though in practice only the phospho-Ser642 antibody was sensitive and phospho-specific (Fig. 2 and [supplemental Fig. S2](#)). Antibody to immunoprecipitate endogenous SMAUG2 from cells and tissues was also generated. The signals from these antibodies were

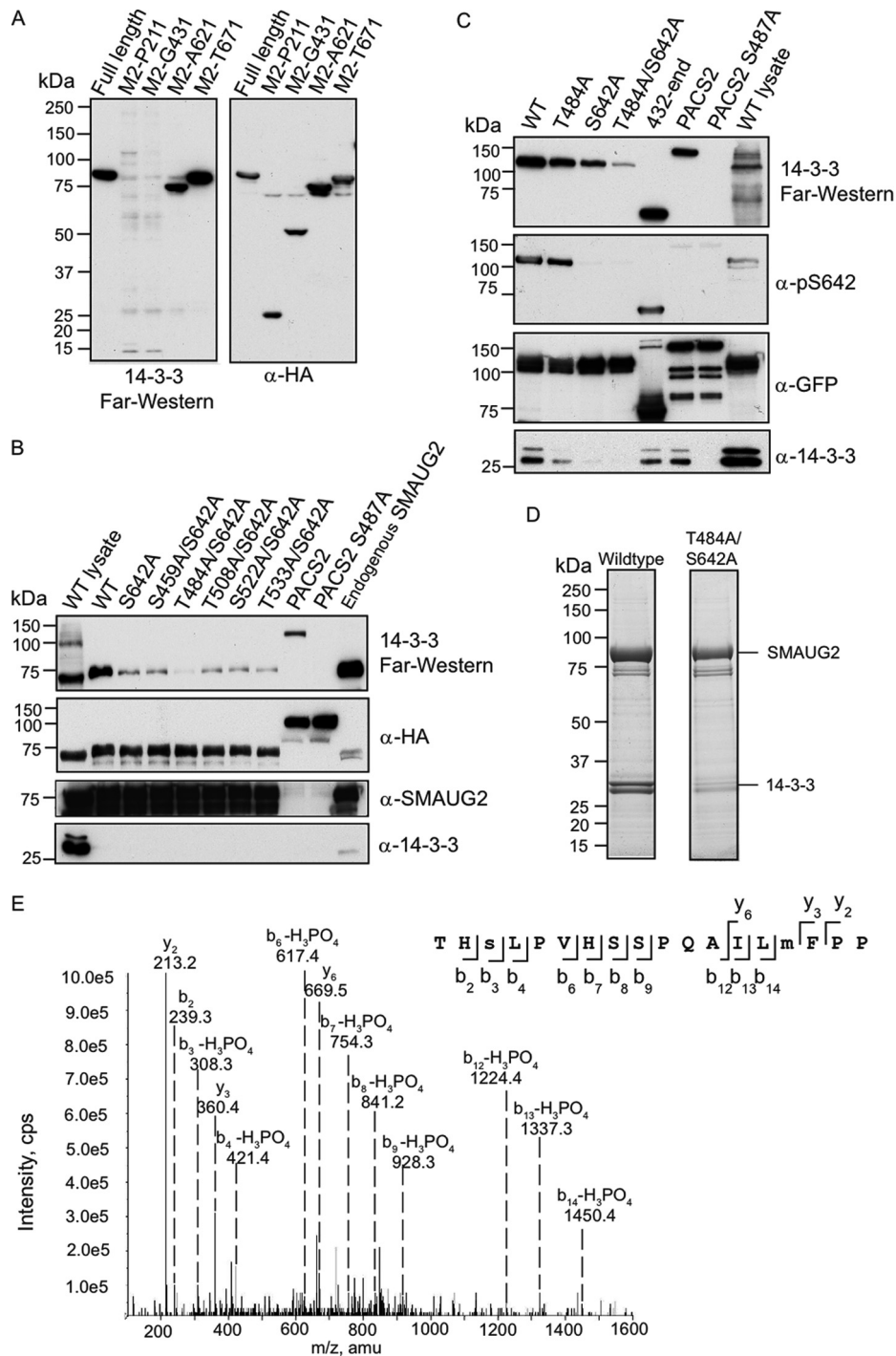


FIG. 4. The phosphorylation-dependent binding of 14-3-3s to SMAUG2. *A*, Analysis of the 14-3-3 binding of truncated SMAUG2 proteins. HEK293 cells were transfected to express the truncated HA-SMAUG2 proteins indicated. Immunoprecipitations were performed with anti-HA antibodies and 14-3-3 binding was assessed using the DIG-14-3-3 Far Western overlay assay. *B*, 14-3-3 binding of alanine mutants of HA-SMAUG2. Recombinant proteins were immunoprecipitated from 1 mg lysate of transfected HEK293 cells and endogenous SMAUG2 from 10 mg untransfected cell lysate, and assayed for their ability to bind to 14-3-3s in a Far Western assay. Copurifying endogenous 14-3-3s were detected with the K19 pan-14-3-3 antibody. PACS2 protein that binds 14-3-3s and mutant PACS2 that does not bind 14-3-3s (1) were positive and negative controls, respectively. *C*, Contribution of phosphorylated Ser642 of SMAUG2 to 14-3-3 binding. GFP-SMAUG2 proteins isolated from 1 mg lysate of transfected HEK293 cells were analyzed with a pSer642-SMAUG2 phosphospecific antibody, 14-3-3 Far Western assay and for coprecipitation of endogenous 14-3-3s. *D*, Tandem affinity purification of GFP-TAP-SMAUG2 proteins. Stable cell lines were generated to express the GFP-TAP proteins at close to endogenous levels when induced with tetracycline (30 ng/ml) for 16 h. Tandem affinity-purified proteins were separated by SDS-PAGE, stained with Coomassie colloidal blue, excised and digested with trypsin for mass fingerprint

consistent with Ser642 being phosphorylated on both recombinant and endogenous cellular SMAUG2 (Fig. 4B and 4C). Furthermore, the endogenous SMAUG2 was confirmed to robustly bind to 14-3-3, both in Far-Western assays and by coimmunoprecipitation of the endogenous 14-3-3s (Fig. 4B).

Still lacking direct proof that the putative 14-3-3-binding sites are phosphorylated, stable cell lines were created expressing forms of SMAUG2, with and without Thr484A/Ser642Ala double mutation, for TAP of the protein and comparative mass spectrometric analysis of phosphopeptides. This experiment confirmed that 14-3-3 binding required Thr484 and Ser642 (Fig. 4D). The predicted tryptic peptide encompassing Ser642 would be 56 residues long, which is not optimal for mass spectrometric analysis, possibly explaining why phosphorylation of this residue has not been reported previously. We therefore performed a double digest of the isolated SMAUG2 using trypsin followed by AspN, resulting in identification of a singly phosphorylated peptide encompassing residues Thr640 to Pro657 (Fig. 4E). The MS/MS spectrum of this phosphopeptide narrowed down the phosphorylated residue to Ser642 (Fig. 4E). Together with the data from the phosphospecific phosphoSer642 antibody, it therefore seems most likely that Ser642 is a phosphorylated 14-3-3-binding site. Although Thr484 is a potential second 14-3-3-binding site, the phosphorylation status of this site remains unknown.

Kinesin Light Chain (KLC) Isoforms—Kinesin is a heterotrimer of two heavy (KHC/KIF5B) and two light (KLC) chains, which exist as multiple isoforms (KLC1 variants, KLC2, KLC3, and KLC4). As a group, these are the most commonly identified proteins across the high-throughput 14-3-3-binding studies summarized here (Fig. 1, [supplemental Table S1](#)).

As expected from previous results (13, 20), Ser575Ala mutation abolished 14-3-3 binding to KLC2. A second 14-3-3-binding site had to exist on KLC2 however, because when various AGC and CAMK kinases were tested for their ability to phosphorylate KLC2 and promote its binding of 14-3-3, we found that MAPKAP kinase 2 phosphorylated Ser575 *in vitro*, but the phosphorylated protein did not bind to 14-3-3 (not shown). In contrast, PKA, AMPK and AMPK-related kinases (Brsk1, Brsk2, QSK, QIK, SIK, Mark1, Mark2, Mark3/C-TAK, Mark4, and Melk, but not Nuak1 and Nuak2) phosphorylated Ser575 and induced binding to 14-3-3 (Fig. 5 and data not shown), which meant that a further residue(s) phosphorylated by these kinases is also essential for 14-3-3 binding.

To pinpoint the second 14-3-3 binding site, GST-KLC2 was phosphorylated *in vitro* with AMPK in the presence of Mg[γ - 32 P]ATP. Tryptic digests of the 32 P-labeled protein were separated by HPLC and contained one major radiolabeled

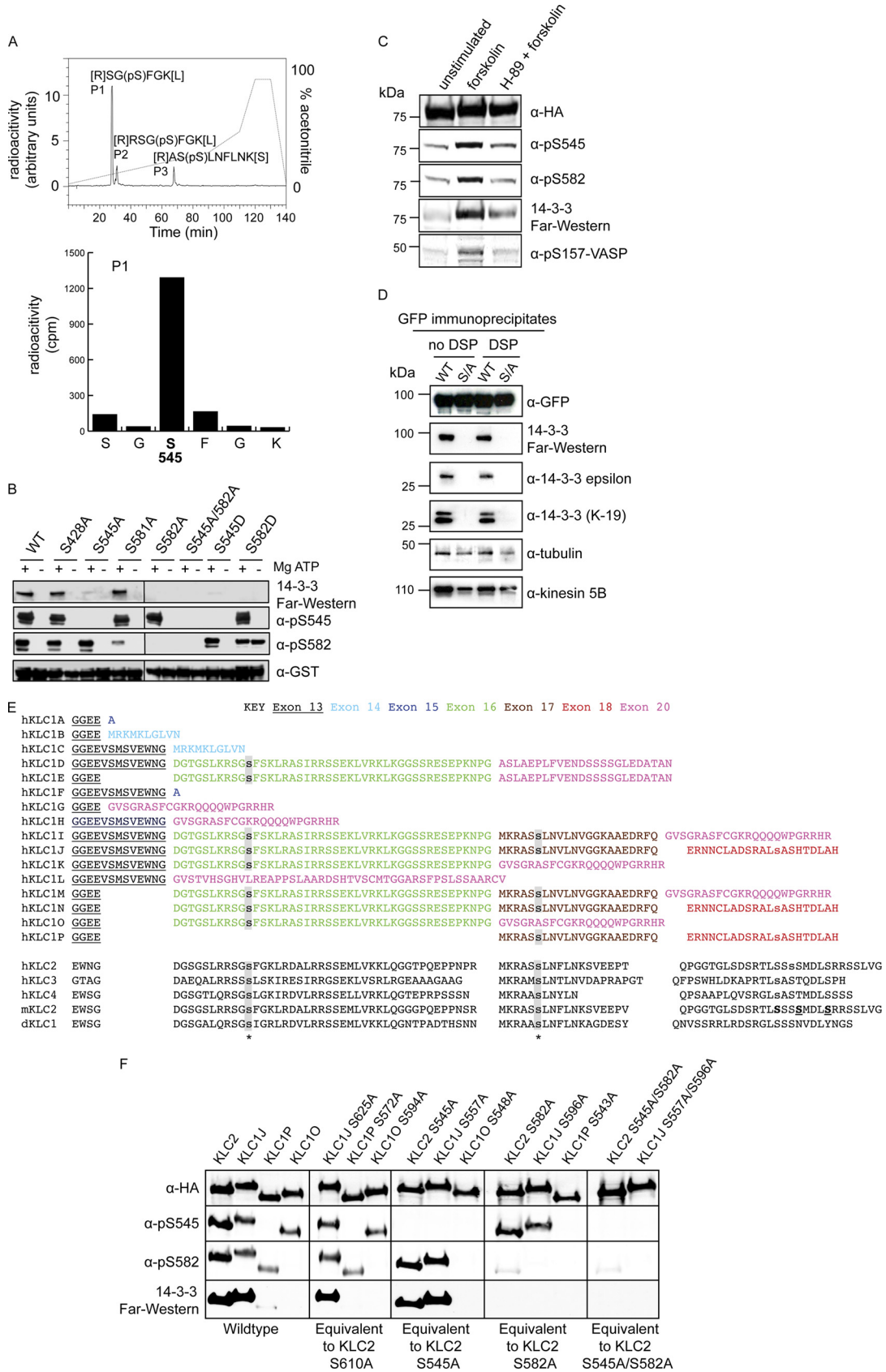
peptide, P1, and two minor radiolabeled peptides P2 and P3 (Fig. 5A). Using mass spectrometry and radioactive solid phase sequencing, P1 was identified as [R]SG(pS)FGK[L] and P2 as [R]RSG(pS)FGK[L] where pS in both cases represents phosphorylated Ser545. P3 was tentatively identified as [R]AS(pS)LNFLNK[S] where the phosphorylated residue is Ser582, and this assignment was supported by mass spectrometric and radioactive Edman degradation analysis of an AspN digest (not shown). Consistent with phosphorylation of both Ser545 and Ser582 of KLC2 contributing to its 14-3-3 binding, a Ser545Ala mutant of KLC2 could be phosphorylated *in vitro* by AMPK on Ser582, but did not bind to 14-3-3 (Fig. 5B). Reciprocally, a Ser582Ala mutant of KLC2 could be phosphorylated by AMPK on Ser545, but did not bind to 14-3-3. Asp substitutions of Ser545 and Ser582 did not mimic the phosphorylated residues for 14-3-3 binding (Fig. 5B).

KLC2 was phosphorylated on both Ser545 and Ser582 when extracted from HEK293 cells (Fig. 2). In HEK293 cells, KLC2 binding to 14-3-3 was not promoted by activators of the AMPK, indicating that AMPK is not a physiological KLC2 kinase (not shown). However, the adenylate cyclase activator forskolin and cell-permeable dibutyryl-cAMP strongly promoted Ser545 and Ser582 phosphorylation and 14-3-3 binding, and the nonspecific PKA inhibitor H-89 blocked these effects (Fig. 5C and data not shown). These findings are consistent with PKA phosphorylating Ser545 and Ser582 in cells.

As expected from the *in vitro* experiment (Fig. 5B), mutation of Ser545 and/or Ser582 abolished the binding of 14-3-3 to KLC2. For example, when GFP-KLC2 was isolated from lysates of transfected cells, 14-3-3 proteins were identified only for the wild-type protein and not a Ser545Ala/Ser582Ala double mutant (Fig. 5D). In contrast, KHC/KIF5B was co-purified with both forms of KLC2 (Fig. 5D). These findings are consistent with the heavy chains being commonly identified in 14-3-3-affinity purification experiments (Fig. 1) because they interact with 14-3-3s indirectly via phosphorylated KLC isoforms.

Aligning the C-terminal sequences of various KLCs (Fig. 5E) showed that residues corresponding to Ser545 and Ser582 are present in both KLC3 and KLC4, explaining why these proteins bind to 14-3-3 (Fig. 1). There is considerable variation in the C-terminal region of KLC1, with four of the known human splice variants harboring a match for Ser545 in a region expressed from exon 16 (KLC1D, E, K, and O), one variant containing the site corresponding to Ser582 expressed from exon 17 (KLC1P), four isoforms with matches for both Ser545 and Ser582 (KLC1I, J, M, and N, expressing both exons 16 and 17) and seven with neither (KLC1A, B, C, F, G, H, and L) (Fig. 5E). These observations prompted us to

identification. The doublet running at ~30 kDa with wild type, but missing in the T484A/S642A SMAUG2 mutant purification, was identified as 14-3-3. *E*, Mass spectrometric identification of phosphorylated Ser642 in recombinant SMAUG2. The MS/MS spectrum shows b- and y- ions resulting from CID fragmentation of THSLPVHSSPQAILMFPP. These data suggest phosphorylation of the third serine in the peptide (Ser642 in SMAUG2) with an ion score of 55 where individual ion scores >33 indicate identity or extensive homology ($p < 0.05$).



test the 14-3-3 binding capacity of three KLC1 variants (Fig. 5F). KLC1J, with residues corresponding to both Ser545 and Ser582 (Ser557, Ser596, respectively), bound 14-3-3s as strongly as KLC2, and similar to KLC2 both single and double Ser to Ala mutants abolished the interaction (Figs. 2 and 5F). In contrast, KLC1P, harboring only the Ser582 equivalent (Ser543) showed only trace binding to 14-3-3. KLC1O, with a Ser545 equivalent site (Ser548) showed no 14-3-3 binding. The cross-reactivity of KLC2 phosphospecific antibodies with the KLC1 variants enabled us to confirm that, as with KLC2, both pSer545 and pSer582 equivalents are required for optimal 14-3-3 binding (Fig. 5F).

In summary, 14-3-3s bind directly to isoforms of KLC1 such as KLC1J, and to KLC2, KLC3 and KLC4, when phosphorylated on sites equivalent to Ser545 and Ser582 in KLC2.

DISCUSSION

The retrieval and handling of protein interaction data is challenging. Despite general efforts in data organization and sharing (40), much information is spread across databases and it is often difficult for the researcher to identify and retrieve a subset of protein-protein interactions from the literature to compare with their own data. Here, we organized published data on interactions of 14-3-3s with individual proteins for submission to the MINT database, as a resource for the community interested in this family of proteins.

In addition, published high-throughput proteomics data on 14-3-3-binding proteins were drawn together from multiple sources and visually represented in VisANT graphs to facilitate its exploration. The VisANT visualization shows that each experiment identifies new proteins, but also misses proteins identified in other studies, even comparing studies using same cell type and similar experimental procedures. To some extent, this situation is an understandable consequence of the state-of-the-art in mass spectrometry. A solution to this problem could be to make inclusion lists of validated 14-3-3-binding proteins to instruct instruments to specifically monitor ion masses for the corresponding peptides, and exclusion lists for the machine to ignore. Reiterations of biochemical validation and high-throughput experiments (in both “inclusion list” and open “discovery” modes) will improve the robustness of mass spectrometry for tracking the dynamics of the 14-3-3-phosphoproteome in response to extracellular stimuli, drugs, and diseases.

However, the VisANT graphs starkly highlighted the sparsity of validated proteins that could be used to make such inclusion lists. To improve this situation, we therefore made a major push to extend the validated data sets. Recent advances that helped these validation experiments are the databases of experimentally identified phosphorylated residues (<http://phospho.elm.eu.org/> and <http://www.phosphosite.org>), from which to identify sites of potential interest guided by the

FIG. 5. The phosphorylation-dependent binding of 14-3-3s to kinesin light chain isoforms. *A*, To identify *in vitro* AMPK-phosphorylated sites on GST-KLC2 that promote binding to 14-3-3s, GST-KLC2 was phosphorylated by AMPK *in vitro* with Mg[γ - 32 P]ATP. A sample was checked for binding to 14-3-3 in a Far Western assay (similar to Fig. 5B, WT), and the remainder digested with trypsin and run on HPLC with the indicated gradient of acetonitrile in 0.1% trifluoroacetic acid. The 32 P trace shows three phosphorylated peptides P1, P2, and P3, which were identified by mass spectrometry to be singly phosphorylated peptides with the amino acid sequences shown. The recovery of 32 P from HPLC was 87%. The phosphorylated residue in P3 was not pinpointed in this experiment, but other data (see text) are consistent with it being Ser582. The *bottom* panel shows that a release of radioactive inorganic phosphate at the third cycle of solid-phase Edman degradation of P1 revealed Ser545 as the phosphorylated residue in that peptide (performed as in (49)). *B*, 14-3-3 binding to GST-KLC2 phosphorylated *in vitro* with AMPK and the effects of Ala and Asp substitutions of Ser residues. Proteins were incubated with AMPK with and without MgATP, and subject to 14-3-3 Far Western binding assay, and immunoblotting with antiphosphoSer545 and antiphosphoSer582, with anti-GST as loading control. In addition to the phosphoSer545 and phosphoSer582 14-3-3 binding sites identified here (see text), mutations of the adjacent Ser581 and also Ser428 (reported to be phosphorylated (<http://www.phosphosite.org>)) and within a Rxx(pS)xP sequence that looks like a 14-3-3-binding motif) were tested, giving no indication that these sites are involved in 14-3-3 binding. As an aside, note that in contrast to 14-3-3, the pSer582 antibody recognizes KLC2 with Asp as a phosphomimetic in place of pSer582. In contrast, the antiphosphoSer545 antibody does not recognize Asp545. Also, mutation of the neighboring residue Ser581 to Ala reduces the ability of the pSer582 antibody, but not 14-3-3, to recognize pSer582. *C*, HA-KLC2 was isolated from transfected HEK293 cells that were serum deprived for 5 h, incubated with or without H-89 (30 μ M for 30 min), and stimulated with the adenylate cyclase activator forskolin (20 μ M for 30 min). The HA-KLC2 was probed for binding to antiphosphoSer545-KLC2, antiphosphoSer582-KLC2 and DIG-14-3-3. The PKA-phosphorylation of Ser157 on VASP was monitored to assess the activation of PKA. *D*, Wild-type and Ser545Ala/Ser582Ala forms of GFP-KLC2 were isolated from lysates of transfected HEK293 cells in the presence and absence of 2.5 mg/ml dithiobis[succinimidyl propionate] (DSP) to stabilize any labile interactions and assayed for direct binding to 14-3-3 in a Far Western, and for the presence of associated proteins with the indicated antibodies. *E*, C-terminal sequences of KLC2 from various species aligned, together with human KLC3 and KLC4 and the C-terminal splice variants of human KLC1 (KNS2 gene; Ensembl ENST00000303439) as reported previously (50). The asterisks align with the positions shaded in gray of Ser545 and Ser582 in human KLC2. Residues in lowercase letters have been shown to be phosphorylated here and elsewhere (<http://www.phosphosite.org>). Underlined residues (Ser611, Ser615) on mouse KLC2 were proposed as GSK3 sites (51); with the preceding bold S proposed as a priming site, though we note that Ser615 has not been shown to be phosphorylated and our attempts to phosphorylate KLC2 with GSK3 *in vitro* and *in vivo*, in experiments using priming kinases and GSK3 inhibitors, were unsuccessful (not shown, including experiments with Adam Cole, University of Dundee). Accession numbers are: hKLC1 Q07866 (human), hKLC2 Q9H0B6 (human), hKLC3 Q6P597 (human), hKLC4 Q9NSK0 (human), mKLC2 O88448 (mouse) and dKLC1 Q7ZVT4 (Zebra fish, *Danio rerio*). *F*, Wild type and mutant HA-tagged KLC1 and KLC2 proteins were immunoprecipitated from HEK293 cells probed with antiphosphoSer545-KLC2, antiphosphoSer582-KLC2 and by Far Western with DIG-14-3-3.

specificities identified from published 14-3-3-binding sites (1), and the GFP-Trap reagent for clean isolation of GFP-tagged proteins from lysates of transfected cells is also useful. Nevertheless, validation is still laborious, requiring a variety of strategies depending on the characteristics of individual phosphorylation sites and proteins. For example, phosphorylated Ser642 of SMAUG2 was identified only by using a phospho-specific antibody and when a trypsin/AspN double digest generated a phosphopeptide within the mass range for analysis.

As well as enhancing datasets to underpin 14-3-3-phosphoproteomics, our findings also point to interesting biology for future discovery. For example, concerns that 14-3-3-affinity purified proteins might be contaminated with mitochondria and ER proteins were not borne out with those proteins tested. 14-3-3 binds to a site in the cytoplasmic side of the ER-tethered protein REEP4 that is conserved in the REEP1 protein, whose mutation causes hereditary spastic paraplegia 31 (9, 26). 14-3-3 must bind to ISCU in the cytoplasm, which is compatible with the cytoplasmic localization of 14-3-3 proteins, because the phosphorylated binding site(s) are in the mitochondrial import sequence of ISCU that is cleaved off when the protein enters the mitochondria. Also, 14-3-3s bind to a site in the cytoplasmic part of mitochondrial fission factor (Fig. 3). Given the central roles of 14-3-3s in upregulating glucose uptake and glycolysis (41, 42), it will be interesting to determine how 14-3-3 binding to mitochondrial proteins influences the balance between mitochondrial and cytoplasmic metabolism, which is commonly deregulated in cancers and other diseases. Indeed, mRNA processing defects in ISCU cause a myopathy with exercise intolerance and lactic acidosis, showing how mitochondrial defects can have secondary effects on cytoplasmic metabolism (43–45).

Pairs of 14-3-3-binding sites sometimes lie either side of a functional domain on a target protein, and interestingly Thr484 and Ser642 of SMAUG2 flank what is predicted to be a globular domain by GlobPlot analysis (<http://globplot.embl.de/>), but whose function is unknown (Table II). Thr484 and Ser642 are conserved across the vertebrate forms of SMAUG2, but not the sequences from invertebrates such as *Drosophila* where the function of Smaug is better defined. Other than 14-3-3s no other proteins were identified to bind to SMAUG2 however, and one possibility is that 14-3-3 binding modulates SMAUG2 binding to mRNAs. For DBNL (actin-binding protein 1), the 14-3-3 binding sites flank a site of proteolysis by calpain 2, which may influence formation of cellular dorsal ruffles (46).

Kinesin is a motor complex that transports proteins along microtubules in the anterograde direction toward the peripheries of cells. The motor action of the paired KHCs “walking” along microtubules has been dissected in exquisite detail, and although KLCs are less well understood they inhibit the KHC motor in the absence of cargo and contribute to cargo loading, with different KLC variants specifying which cargoes are

loaded up for trafficking (47). Our finding that 14-3-3s bind to phosphorylated residues on KLC2, KLC3, KLC4 and isoforms of KLC1 containing sequences expressed from exon 16 and/or exon 17, suggest that 14-3-3s may be involved in specifying cargo loading/unloading. A KLC1 variant that is enriched on mitochondria and rough endoplasmic reticulum, KLC1B, has neither of the 14-3-3 binding sites identified in the present study, whereas variants located on the Golgi apparatus, KLC1D and KLC1E lack Ser582 but contain Ser545 (47). The specific cargoes of the KLC1 isoforms that contain both 14-3-3-binding sites have not been defined however, and one possibility is that the 14-3-3s are themselves the cargoes, contributing to the roles of 14-3-3s in cell polarity (48).

Acknowledgments—We thank Becky Tillotson and Christopher Ford for contributing to Figs. 2 and 3, the antibody purification team of the DSTT coordinated by Hilary McLauchlan and James Hastie for generation and purification of antibodies, and Kirsten Mcleod and Janis Stark for tissue culture support.

* This work was supported by The Cunningham Trust, U.K. Medical Research Council via a Developmental Pathway Funding scheme award and core funding, and companies who support the Division of Signal Transduction Therapy (DSTT) at the University of Dundee, namely AstraZeneca, Boehringer Ingelheim, GlaxoSmithKline, Merck Serono and Pfizer.

§ This article contains [supplemental Figs. S1 and S2 and Tables S1 to S3](#).

§ To whom correspondence should be addressed: MRC Protein Phosphorylation Unit, College of Life Sciences, University of Dundee, James Black Centre, Dow Street, Dundee DD1 5EH, Scotland, U.K. Tel.: 44-1382-385766; Fax: 44-1382-223778; E-mail: c.mackintosh@dundee.ac.uk.

¶ These authors made equally important contributions and are joint first authors.

REFERENCES

- Johnson, C., Crowther, S., Stafford, M. J., Campbell, D. G., Toth, R., and MacKintosh, C. (2010) Bioinformatic and experimental survey of 14-3-3-binding sites. *Biochem. J.* **427**, 69–78
- Dubois, F., Vandermoere, F., Gernez, A., Murphy, J., Toth, R., Chen, S., Geraghty, K. M., Morrice, N. A., and MacKintosh, C. (2009) Differential 14-3-3 affinity capture reveals new downstream targets of phosphatidylinositol 3-kinase signaling. *Mol. Cell Proteomics* **8**, 2487–2499
- Larance, M., Rowland, A. F., Hoehn, K. L., Humphreys, D. T., Preiss, T., Guilhaus, M., and James, D. E. (2010) Global phosphoproteomics identifies a major role for AKT and 14-3-3 in regulating EDC3. *Mol. Cell Proteomics* **9**, 682–694
- Yip, M. F., Ramm, G., Larance, M., Hoehn, K. L., Wagner, M. C., Guilhaus, M., and James, D. E. (2008) CaMKII-mediated phosphorylation of the myosin motor Myo1c is required for insulin-stimulated GLUT4 translocation in adipocytes. *Cell Metab.* **8**, 384–398
- Alexander, R. D., and Morris, P. C. (2006) A proteomic analysis of 14-3-3 binding proteins from developing barley grains. *Proteomics* **6**, 1886–1896
- Huang, W. G., Cheng, A. L., Chen, Z. C., Peng, F., Zhang, P. F., Li, M. Y., Li, F., Li, J. L., Li, C., Yi, H., Li, X. H., Yi, B., and Xiao, Z. Q. (2010) Targeted proteomic analysis of 14-3-3sigma in nasopharyngeal carcinoma. *Int. J. Biochem. Cell Biol.* **42**, 137–147
- He, Y. F., Bao, H. M., Xiao, X. F., Zuo, S., Du, R. Y., Tang, S. W., Yang, P. Y., and Chen, X. (2009) Biotin tagging coupled with amino acid-coded mass tagging for efficient and precise screening of interaction proteome in mammalian cells. *Proteomics* **9**, 5414–5424
- Wilker, E., and Yaffe, M. B. (2004) 14-3-3 Proteins—a focus on cancer and human disease. *J. Mol. Cell Cardiol.* **37**, 633–642

9. Züchner, S., Wang, G., Tran-Viet, K. N., Nance, M. A., Gaskell, P. C., Vance, J. M., Ashley-Koch, A. E., and Pericak-Vance, M. A. (2006) Mutations in the novel mitochondrial protein REEP1 cause hereditary spastic paraplegia type 31. *Am. J. Hum. Genet.* **79**, 365–369
10. Angrand, P. O., Segura, I., Völkel, P., Ghidelli, S., Terry, R., Brajenovic, M., Vintersten, K., Klein, R., Superti-Furga, G., Drewes, G., Kuster, B., Bouwmeester, T., and Acker-Palmer, A. (2006) Transgenic mouse proteomics identifies new 14-3-3-associated proteins involved in cytoskeletal rearrangements and cell signaling. *Mol. Cell Proteomics* **5**, 2211–2227
11. Chang, I. F., Curran, A., Woolsey, R., Quilici, D., Cushman, J. C., Mittler, R., Harmon, A., and Harper, J. F. (2009) Proteomic profiling of tandem affinity purified 14-3-3 protein complexes in *Arabidopsis thaliana*. *Proteomics* **9**, 2967–2985
12. Ewing, R. M., Chu, P., Elisma, F., Li, H., Taylor, P., Climie, S., McBroom-Cerajewski, L., Robinson, M. D., O'Connor, L., Li, M., Taylor, R., Dharsee, M., Ho, Y., Heilbut, A., Moore, L., Zhang, S., Ornatsky, O., Bukhman, Y. V., Ethier, M., Sheng, Y., Vasilescu, J., Abu-Farha, M., Lambert, J. P., Duester, H. S., Stewart, II, Kuehl, B., Hogue, K., Colwill, K., Gladwish, K., Muskat, B., Kinach, R., Adams, S. L., Moran, M. F., Morin, G. B., Topaloglu, T., and Figeys, D. (2007) Large-scale mapping of human protein-protein interactions by mass spectrometry. *Mol. Syst. Biol.* **3**, 89
13. Ichimura, T., Wakamiya-Tsuruta, A., Itagaki, C., Taoka, M., Hayano, T., Natsume, T., and Isobe, T. (2002) Phosphorylation-dependent interaction of kinesin light chain 2 and the 14-3-3 protein. *Biochemistry* **41**, 5566–5572
14. Jin, J., Smith, F. D., Stark, C., Wells, C. D., Fawcett, J. P., Kulkarni, S., Metalnikov, P., O'Donnell, P., Taylor, P., Taylor, L., Zougman, A., Woodgett, J. R., Langeberg, L. K., Scott, J. D., and Pawson, T. (2004) Proteomic, functional, and domain-based analysis of in vivo 14-3-3 binding proteins involved in cytoskeletal regulation and cellular organization. *Curr. Biol.* **14**, 1436–1450
15. Kakiuchi, K., Yamauchi, Y., Taoka, M., Iwago, M., Fujita, T., Ito, T., Song, S. Y., Sakai, A., Isobe, T., and Ichimura, T. (2007) Proteomic analysis of in vivo 14-3-3 interactions in the yeast *Saccharomyces cerevisiae*. *Biochemistry* **46**, 7781–7792
16. Meek, S. E., Lane, W. S., and Piwnicka-Worms, H. (2004) Comprehensive proteomic analysis of interphase and mitotic 14-3-3-binding proteins. *J. Biol. Chem.* **279**, 32046–32054
17. Moorhead, G., Douglas, P., Cotellet, V., Harthill, J., Morrice, N., Meek, S., Deiting, U., Stitt, M., Scarabel, M., Aitken, A., and MacKintosh, C. (1999) Phosphorylation-dependent interactions between enzymes of plant metabolism and 14-3-3 proteins. *Plant J.* **18**, 1–12
18. Paul, A. L., Liu, L., McClung, S., Laughner, B., Chen, S., and Ferl, R. J. (2009) Comparative interactomics: analysis of arabidopsis 14-3-3 complexes reveals highly conserved 14-3-3 interactions between humans and plants. *J. Proteome Res.* **8**, 1913–1924
19. Pauly, B., Lasi, M., MacKintosh, C., Morrice, N., Imhof, A., Regula, J., Rudd, S., David, C. N., and Böttger, A. (2007) Proteomic screen in the simple metazoan Hydra identifies 14-3-3 binding proteins implicated in cellular metabolism, cytoskeletal organization and Ca²⁺ signalling. *BMC Cell Biol.* **8**, 31
20. Pozuelo Rubio, M., Geraghty, K. M., Wong, B. H., Wood, N. T., Campbell, D. G., Morrice, N., and Mackintosh, C. (2004) 14-3-3-affinity purification of over 200 human phosphoproteins reveals new links to regulation of cellular metabolism, proliferation and trafficking. *Biochem. J.* **379**, 395–408
21. Puri, P., Myers, K., Kline, D., and Vijayaraghavan, S. (2008) Proteomic analysis of bovine sperm YWHA binding partners identify proteins involved in signaling and metabolism. *Biol. Reprod.* **79**, 1183–1191
22. Schoonheim, P. J., Veiga, H., Pereira Dda, C., Friso, G., van Wijk, K. J., and de Boer, A. H. (2007) A comprehensive analysis of the 14-3-3 interactome in barley leaves using a complementary proteomics and two-hybrid approach. *Plant Physiol.* **143**, 670–683
23. Wilker, E. W., van Vugt, M. A., Artim, S. A., Huang, P. H., Petersen, C. P., Reinhardt, H. C., Feng, Y., Sharp, P. A., Sonenberg, N., White, F. M., and Yaffe, M. B. (2007) 14-3-3sigma controls mitotic translation to facilitate cytokinesis. *Nature* **446**, 329–332
24. Zuo, S., Xue, Y., Tang, S., Yao, J., Du, R., Yang, P., and Chen, X. (2010) 14-3-3 epsilon dynamically interacts with key components of mitogen-activated protein kinase signal module for selective modulation of the TNF-alpha-induced time course-dependent NF-kappaB activity. *J. Proteome Res.* **9**, 3465–3478
25. Liang, S., Yu, Y., Yang, P., Gu, S., Xue, Y., and Chen, X. (2009) Analysis of the protein complex associated with 14-3-3 epsilon by a deuterated-leucine labeling quantitative proteomics strategy. *J. Chromatogr. B Analyt. Technol. Biomed. Life Sci.* **877**, 627–634
26. Park, S. H., Zhu, P. P., Parker, R. L., and Blackstone, C. (2010) Hereditary spastic paraplegia proteins REEP1, spastin, and atlastin-1 coordinate microtubule interactions with the tubular ER network. *J. Clin. Invest.* **120**, 1097–1110
27. Pozuelo-Rubio, M. (2010) Proteomic and biochemical analysis of 14-3-3-binding proteins during C2-ceramide-induced apoptosis. *FEBS J* **277**, 3321–3342
28. Benzinger, A., Muster, N., Koch, H. B., Yates, J. R., 3rd, and Hermeking, H. (2005) Targeted proteomic analysis of 14-3-3 sigma, a p53 effector commonly silenced in cancer. *Mol. Cell Proteomics* **4**, 785–795
29. Ceol, A., Chatr-Aryamontri, A., Licata, L., Peluso, D., Briganti, L., Perfetto, L., Castagnoli, L., and Cesareni, G. (2010) MINT, the molecular interaction database: 2009 update. *Nucleic Acids Res.* **38**, D532–539
30. Aranda, B., Achuthan, P., Alam-Farouque, Y., Armean, I., Bridge, A., Derow, C., Feuermann, M., Ghanbarian, A. T., Kerrien, S., Khadake, J., Kerssemakers, J., Leroy, C., Menden, M., Michaut, M., Montecchi-Palazzi, L., Neuhauser, S. N., Orchard, S., Perreau, V., Roechert, B., van Eijk, K., and Hermjakob, H. (2010) The IntAct molecular interaction database in 2010. *Nucleic Acids Res.* **38**, D525–531
31. Cock, P. J., Antao, T., Chang, J. T., Chapman, B. A., Cox, C. J., Dalke, A., Friedberg, I., Hamelryck, T., Kauff, F., Wilczynski, B., and de Hoon, M. J. (2009) Biopython: freely available Python tools for computational molecular biology and bioinformatics. *Bioinformatics* **25**, 1422–1423
32. Huang da, W., Sherman, B. T., and Lempicki, R. A. (2009) Systematic and integrative analysis of large gene lists using DAVID bioinformatics resources. *Nat. Protoc.* **4**, 44–57
33. Smith, A. C., and Robinson, A. J. (2009) MitoMiner, an integrated database for the storage and analysis of mitochondrial proteomics data. *Mol. Cell Proteomics* **8**, 1324–1337
34. Ahmad, Y., Boisvert, F. M., Gregor, P., Cobley, A., and Lamond, A. I. (2009) NOPdb: Nucleolar Proteome Database–2008 update. *Nucleic Acids Res.* **37**, D181–184
35. Hu, Z., Hung, J. H., Wang, Y., Chang, Y. C., Huang, C. L., Huyck, M., and DeLisi, C. (2009) VisANT 3.5: multi-scale network visualization, analysis and inference based on the gene ontology. *Nucleic Acids Res.* **37**, W115–121
36. Puig, O., Casparly, F., Rigaut, G., Rutz, B., Bouveret, E., Bragado-Nilsson, E., Wilm, M., and Séraphin, B. (2001) The tandem affinity purification (TAP) method: a general procedure of protein complex purification. *Methods* **24**, 218–229
37. Olsen, J. V., de Godoy, L. M., Li, G., Macek, B., Mortensen, P., Pesch, R., Makarov, A., Lange, O., Hornung, S., and Mann, M. (2005) Parts per million mass accuracy on an Orbitrap mass spectrometer via lock mass injection into a C-trap. *Mol. Cell Proteomics* **4**, 2010–2021
38. Williamson, B. L., Marchese, J., and Morrice, N. A. (2006) Automated identification and quantification of protein phosphorylation sites by LC/MS on a hybrid triple quadrupole linear ion trap mass spectrometer. *Mol. Cell Proteomics* **5**, 337–346
39. Lizcano, J. M., Göransson, O., Toth, R., Deak, M., Morrice, N. A., Boudeau, J., Hawley, S. A., Udd, L., Makela, T. P., Hardie, D. G., and Alessi, D. R. (2004) LKB1 is a master kinase that activates 13 kinases of the AMPK subfamily, including MARK/PAR-1. *EMBO J.* **23**, 833–843
40. Orchard, S., Salwinski, L., Kerrien, S., Montecchi-Palazzi, L., Oesterheld, M., Stümpflen, V., Ceol, A., Chatr-aryamontri, A., Armstrong, J., Woolard, P., Salama, J. J., Moore, S., Wojcik, J., Bader, G. D., Vidal, M., Cusick, M. E., Gerstein, M., Gavin, A. C., Superti-Furga, G., Greenblatt, J., Bader, J., Uetz, P., Tyers, M., Legrain, P., Fields, S., Mulder, N., Gilson, M., Niepmann, M., Burgoon, L., De Las Rivas, J., Prieto, C., Perreau, V. M., Hogue, C., Mewes, H. W., Apweiler, R., Xenarios, I., Eisenberg, D., Cesareni, G., and Hermjakob, H. (2007) The minimum information required for reporting a molecular interaction experiment (MIMIX). *Nat. Biotechnol.* **25**, 894–898
41. Chen, S., Murphy, J., Toth, R., Campbell, D. G., Morrice, N. A., and Mackintosh, C. (2008) Complementary regulation of TBC1D1 and AS160 by growth factors, insulin and AMPK activators. *Biochem. J.* **409**, 449–459

42. Pozuelo Rubio, M., Peggie, M., Wong, B. H., Morrice, N., and MacKintosh, C. (2003) 14-3-3s regulate fructose-2,6-bisphosphate levels by binding to PKB-phosphorylated cardiac fructose-2,6-bisphosphate kinase/phosphatase. *EMBO J.* **22**, 3514–3523
43. Mochel, F., and Haller, R. G. (2009) Myopathy with Deficiency of ISCU. In: Pagon, R. A., Bird, T. C., Dolan, C. R., and Stephens, K., eds. *GeneReviews [Internet]*, University of Washington, Seattle
44. Mochel, F., Knight, M. A., Tong, W. H., Hernandez, D., Ayyad, K., Taivasalo, T., Andersen, P. M., Singleton, A., Rouault, T. A., Fischbeck, K. H., and Haller, R. G. (2008) Splice mutation in the iron-sulfur cluster scaffold protein ISCU causes myopathy with exercise intolerance. *Am. J. Hum. Genet.* **82**, 652–660
45. Olsson, A., Lind, L., Thornell, L. E., and Holmberg, M. (2008) Myopathy with lactic acidosis is linked to chromosome 12q23.3–24.11 and caused by an intron mutation in the ISCU gene resulting in a splicing defect. *Hum. Mol. Genet.* **17**, 1666–1672
46. Cortesio, C. L., Perrin, B. J., Bennin, D. A., and Huttenlocher, A. (2010) Actin-binding protein-1 interacts with WASp-interacting protein to regulate growth factor-induced dorsal ruffle formation. *Mol. Biol. Cell* **21**, 186–197
47. Woźniak, M. J., and Allan, V. J. (2006) Cargo selection by specific kinesin light chain 1 isoforms. *EMBO J.* **25**, 5457–5468
48. Bunney, T. D., De Boer, A. H., and Levin, M. (2003) Fusicocin signaling reveals 14-3-3 protein function as a novel step in left-right patterning during amphibian embryogenesis. *Development* **130**, 4847–4858
49. Campbell, D. G., and Morrice, N. A. (2002) Identification of protein phosphorylation sites by a combination of mass spectrometry and solid phase Edman sequencing. *J. Biomol. Tech.* **13**, 119–130
50. McCart, A. E., Mahony, D., and Rothnagel, J. A. (2003) Alternatively spliced products of the human kinesin light chain 1 (KNS2) gene. *Traffic* **4**, 576–580
51. Morfini, G., Szebenyi, G., Elluru, R., Ratner, N., and Brady, S. T. (2002) Glycogen synthase kinase 3 phosphorylates kinesin light chains and negatively regulates kinesin-based motility. *EMBO J.* **21**, 281–293
52. Ren, J., Wen, L., Gao, X., Jin, C., Xue, Y., and Yao, X. (2009) DOG 1.0: illustrator of protein domain structures. *Cell Res.* **19**, 271–273
53. Gandre-Babbe, S., and van der Bliek, A. M. (2008) The novel tail-anchored membrane protein Mff controls mitochondrial and peroxisomal fission in mammalian cells. *Mol. Biol. Cell* **19**, 2402–2412
54. Ye, H., and Rouault, T. A. (2010) Human iron-sulfur cluster assembly, cellular iron homeostasis, and disease. *Biochemistry* **49**, 4945–4956
55. Kollberg, G., and Holme, E. (2009) Antisense oligonucleotide therapeutics for iron-sulphur cluster deficiency myopathy. *Neuromuscul. Disord* **19**, 833–836
56. Tadros, W., Westwood, J. T., and Lipshitz, H. D. (2007) The mother-to-child transition. *Dev. Cell* **12**, 847–849
57. Baez, M. V., and Boccaccio, G. L. (2005) Mammalian Smaug is a translational repressor that forms cytoplasmic foci similar to stress granules. *J. Biol. Chem.* **280**, 43131–43140